frontiers | Frontiers in Materials

TYPE Original Research
PUBLISHED 15 September 2023
DOI 10.3389/fmats.2023.1270865

OPEN ACCESS

EDITED BY
Bing Bai,
Beijing Jiaotong University, China

REVIEWED BY
Chen Peipei,
Beijing University of Civil Engineering and Architecture, China
Yang Gaosheng,
Shanxi Agricultural University, China

*CORRESPONDENCE
Huawei Tong,
faiychen@gzhu.edu.cn

RECEIVED 01 August 2023
ACCEPTED 05 September 2023
PUBLISHED 15 September 2023

CITATION
Chen J, Yuan J, Tong H, Fang Y and Gu R (2023), Mechanism study on the soil mechanical behavior of the mixed soil based on energy multi-scale method. *Front. Mater.* 10:1270865. doi: 10.3389/fmats.2023.1270865

Mechanism study on the soil mechanical behavior of the mixed soil based on energy multi-scale method

Jian Chen[1,2], Jie Yuan[1], Huawei Tong[1]*, Yingguang Fang[3] and Renguo Gu[3]

[1]School of Civil Engineering, Guangzhou University, Guangzhou, China, [2]School of Railway Engineering, Guangzhou Railway Polytechnic, Guangzhou, China, [3]South China University of Technology, Guangzhou, China

The presence of mixed soil is widespread in nature, rendering it susceptible to geological hazards such as landslides, liquefaction, and debris flows. This soil type displays pronounced structural anisotropy due to its diverse mineral composition and the broad range of particle sizes it encompasses across multiple geometric scales. However, there exists an array of conflicting research outcomes concerning the impact of particle composition, size, and content on the mechanical properties of mixed soil. This study delves into the mechanical behavior of mixed soil across varying particle contents and sizes using direct shear testing. Subsequently, the distinctive mechanical responses are dissected by scrutinizing the interplay of particle contact interfaces. Concurrently, the underlying mechanism behind this behavior is explored by examining particle surface adsorption energy through a multi-energy scale approach. In conclusion, the following findings are established: 1) The influence of fine particle content (FC) on mixed soil strength varies according to distinct filling conditions; 2) The contribution to mixed soil strength differs among particles with distinct mineral components; 3) Sand particle size within mixed soil holds no sway over its strength under equivalent mass conditions; 4) The particle surface energy equation derived from the multi-energy scale technique comprehensively elucidates the interplay between particle composition, content, and mechanical behavior in mixed soil.

KEYWORDS

mixed soil, energy multi-scale method, direct shear test, mechanical behavior, contact interface, microstructure, adsorbed water, microscopic forces

1 Introduction

Mixed soil, found extensively in natural contexts such as weathered mountain slopes, alluvial deposits, sea-land interactions, and tailings, holds significant relevance for both human life and engineering endeavors. Within mixed soil, the presence of fine particles interspersed among coarser particles, with distinct geometric scales and mineral compositions, results in complex particle-to-particle contact interfaces. This intricate arrangement contributes to the conspicuous anisotropy characterizing the soil's structure. Disturbingly, the collapse of mixed soil readily triggers substantial deformations and gives rise to geological hazards, including landslides, liquefaction, and mudslides, as illustrated in Figure 1. Notably, research underscores the substantial mechanical divergence between mixed soil and pure sand or clay (Yamamuro and Lade,

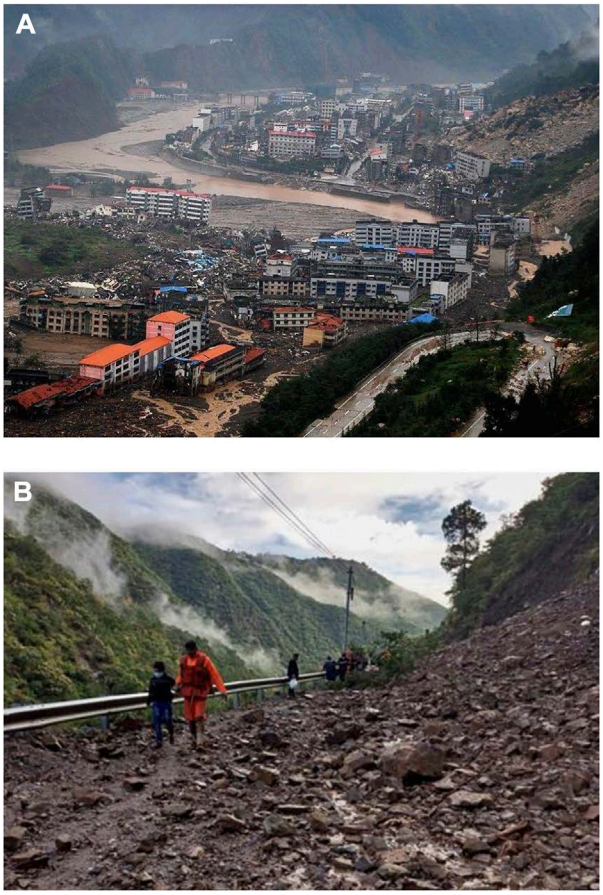

FIGURE 1
Instances of geological hazards in mixed soil. **(A)** Landslides and mudslides post Wenchuan earthquake; **(B)** Landslides induced by rainstorms in East Akhand, India.

1998; Bobei and Lo, 2009; Ke and Chen, 2019; Wei and Yang, 2019; Porcino and Diano, 2020; Bai et al., 2021). To elucidate these differential behaviors, scholars have extensively investigated factors encompassing fine particle content (FC), particle physical attributes, and internal soil structure.

Foremost among these factors, the influence of FC on mixed soil properties garnered early attention. Troncoso and Verdugo (1985) executed cyclic shear tests on tailings with varying mass proportions of silt, showcasing decreased cyclic shear strength with rising silt content. However, Amini and Qi (2000) demonstrated enhanced cyclic resistance in fine-grained sandy soil as FC increased, based on triaxial experiments. Conversely, Polito and Martin (2001) reported an initial decrease followed by an increase in liquefaction resistance with fine-grained sandy soil's FC. Examining the anisotropic effect of sand-silt mixtures, Bahadori and Ghalandarzadeh et al. (2008) identified a trend of decreasing and then increasing anisotropy with silt content. Carraro and Prezzi. (2009) noted variations in critical state friction angle and peak stress of sandy soil due to FC changes, differing based on the properties of the fines. Krim and Arab. (2017) linked reduced liquefaction resistance to increased clay content. Porcino and Diano et al. (2020) established that, upon reaching a threshold fines content at constant porosity, a more contractive behavior emerged, with heightened strain softening as fines content increased. Monkul and Kendir. (2021) documented two tendencies: cyclic resistance ratio (CRR) initially increased and then decreased for small FC values (approximately 5%–10%) within the studied range (FC ≤ 35%); CRR consistently diminished for FC values up to 35%. Li and Liu, (2022) findings exhibited linear growth in cohesion, uniformity coefficient, and curvature coefficient with increasing FC, while friction angle declined. Zuo and Gu. (2023) found that a non-linear decrease in small-strain shear modulus accompanied FC increase to 30%, reaching nearly 50% of clean sand's modulus at maximum FC.

Beyond geometric size, the plasticity of fine particles holds significant sway over mixed soil strength (Lee and Seed, 1967). Carraro and Prezzi. (2009) highlighted elevated critical state friction angle and peak stress as silt content increased within mixed sand, with opposing trends observed for clay. Park and Kim (2013) demonstrated decreased dynamic strength in sand-clay mixtures of differing densities with higher clay plasticity indices. Monkul and Yamamuro (2011), as well as Monkul and Etminan. (2017), underscored the influence of fine particle shape on sandy soil liquefaction. Krim and Arab, (2017) associated both particle shape and FC with mixed soil liquefaction resistance. Zhu and Zhang, (2020) noted that larger particles generated occlusal structures, enhancing friction, while identical-sized sand particles were more prone to sliding. Monkul and Kendir et al. (2021) delineated coarse-fine contacts' impact on overall stress-strain behavior, with fines creating substructures between coarser grains. Chang and Yin et al. (2010) conceived soil as a particle aggregate, where all-direction particle contact dictated stress-strain correlation. Gong and Nie, (2019) quantified different contact types' contributions to residual shear strength, including coordination number and normal contact force. Phan and Bui, (2021) attributed mixed soil shear resistance to particle contact type and proportion, emphasizing fine powder's role in altering sand properties. Allahyari and Maleki (2022) affirmed relative density and confining pressure's substantial impact on maximum shear modulus.

In the domain of FC, fine particles within the 0%–8% range were found to stabilize anisotropic structures and enhance stiffness anisotropy (Gao and Wang, 2015). Sabbar and Chegenizadeh (2017) posited that fine particles create a structure that narrows inter-particle pores, subsequently altering soil liquefaction resistance. Zhu and Zhang (2020) observed larger particles forming occlusal structures, providing greater friction, while particles of uniform size were more susceptible to sliding. Monkul and Kendir et al. (2021) highlighted the role of coarse-fine contacts in shaping soil's stress-strain behavior. Chang and Yin, (2010) regarded soil as an aggregate, where particle contacts in all directions dictated stress-strain relationships. Gong and Nie, (2019) established varying contributions of contact types to residual shear strength, encompassing coordination number and normal contact force. Phan and Bui, (2021) attributed mixed soil shear resistance to particle contact type and proportion, emphasizing fine powder's role in altering sand properties. Allahyari and Maleki (2022) affirmed relative density and confining pressure's substantial impact on maximum shear modulus.

Mixed soil, being a confluence of varying particle sizes and mineral compositions, exhibits mechanical behavior significantly influenced by particle geometry, mineral composition, and content.

TABLE 1 The basic information of the experimental materials.

Object	Average diameter (mm)	Specific gravity	Plastic limit	Liquid limit	Plasticity index	Minerals
Bentonite	0.015	2.53	48%	213.50%	165.5	Quartz 0.8%, cristobalite 0.39%, Montmorillonite 91.7%, clinoptilolite 1.7%, Sodalite 2.0%
Quartz sand	0.5,0.7,0.9,1.5	2.63	--	-	--	--

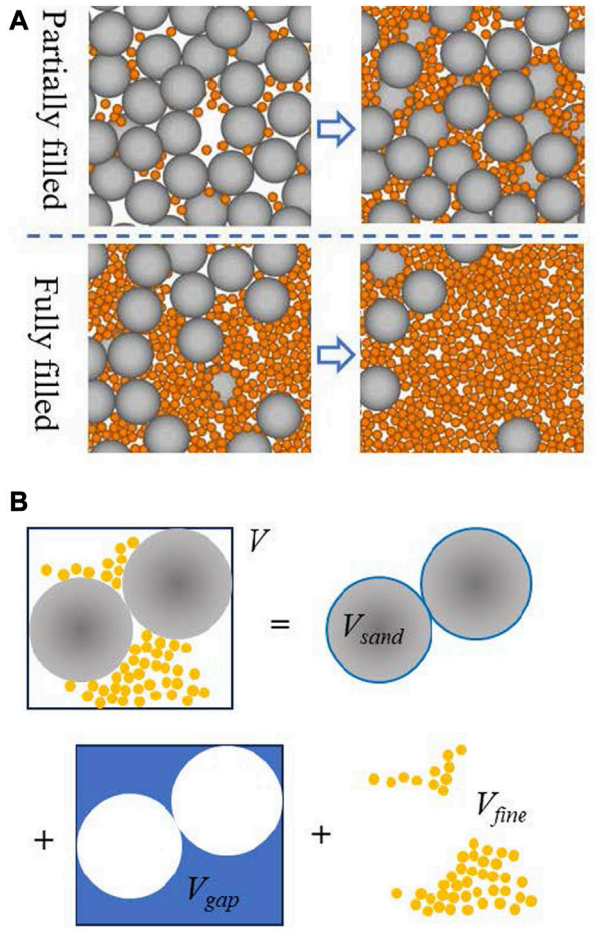

FIGURE 2
Schematic diagram of sample preparation method. **(A)** Schematic representation of fabric cases; **(B)** Schematic diagram of sample method.

FIGURE 3
Test on the mechanical behavior of mixed soil. **(A)** Sample of mixed soil; **(B)** Experimental instrument.

Prior research has provided insight into certain aspects of this behavior via internal structure analysis. However, the precise mechanisms remain unclear, resulting in conflicting findings across mixed soil studies. Given these challenges, this paper endeavors to dissect the mechanical behavior of diverse mixed soil samples via experimentation. The ensuing analysis encompasses FC, particle composition, and size, scrutinizing their contribution to microstructural deformation and particle interface properties. Subsequently, utilizing an energy scale approach, the paper delves into the mechanism behind this behavior at the micro-level, particularly focusing on particle surface energy and contact interfaces. This comprehensive approach aims to draw valuable conclusions from the investigation.

2 Experimental investigation of mechanical behavior in mixed soil

2.1 Test configuration

In this experimental study, we systematically investigate how various factors, including particle size, mineral composition, and particle content, influence the mechanical behavior of mixed soil.

TABLE 2 Sample preparation plan and experimental plan.

No.	M_{sand}(g)	V_{sand} (cm^3)	$M_{wet\ fines}$(g)	$V_{wet\ fines}$ (cm^3)	CF (%)	Vertical load	d_{sand}
ZJ-03V	91.90	34.55	12.79	7.63	0.13	100kPa, 150kPa, 200kPa, 250kPa	0.5 mm, 0.7 mm, 0.9 mm, 1.5 mm.
ZJ-04V	91.90	34.55	17.05	10.18	0.17		
ZJ-05V	91.90	34.55	21.31	12.72	0.21		
ZJ-06V	91.90	34.55	25.58	15.26	0.25		
ZJ-07V	91.90	34.55	29.84	17.81	0.30		
ZJ-08V	91.90	34.55	34.10	20.35	0.34		
ZJ-1M	91.90	34.55	40.95	24.44	0.41		
ZJ-09M	82.71	31.09	48.42	28.90	0.48		
ZJ-08M	73.52	27.64	54.21	32.35	0.54		
ZJ-07M	64.33	24.18	59.99	35.81	0.60		
ZJ-06M	55.14	20.73	65.78	39.26	0.65		
ZJ-03M	27.57	10.36	83.15	49.63	0.83		

Our experimental setup involves quartz sand as the coarse-grained component and wet bentonite powder as the fine-grained component. The quartz sand was screened using sieves with pore sizes of 0.4 mm–0.6 mm, 0.6 mm–0.8 mm, 0.8 mm–1.0 mm, and 1.0 mm–2.0 mm, respectively. So, the average diameters of the quartz sand particles are 0.5 mm, 0.7 mm, 0.9 mm, and 1.5 mm. Since bentonite is purchased commercially, its mineral composition was tested to ensure that the clay mineral content meets the requirements. Detailed information about these materials is provided in Table 1.

Figure 2A illustrates the two predominant states that can be observed in mixed soil samples: one in which there are sufficient fine particles to completely fill the gaps between coarse particles, resulting in minimal contact between the coarse grains, and another where there are enough coarse grains, causing the fine grains to partially fill the gaps. These states play a crucial role in determining the mechanical behavior of the soil (Yin and Zhao, 2014; De Frias Lopez and Silfwerbrand et al., 2016).

To investigate the mechanical behavior of mixed soil under different conditions as shown in Figure 2A, we prepare samples by carefully controlling the content of fine and sand particles. The sample preparation process is outlined in Figure 2B. Each sample is prepared within a ring knife with a diameter of 6.18 cm and a height of 2 cm, as depicted in Figure 3. The volume of the ring knife is denoted as V.

The sample preparation process proceeds as follows:

1. Calculate the mass (M_{0sand}) and volume (V_{0sand}) of the sand in the ring knife based on the natural bulk density of the sand.
2. Determine the gap volume (V_{gap}) between the sand particles.
3. Gradually fill the gaps by controlling the volume of fine particles (V_{fine}), such as V_{fine} = 0.3Vgap, V_{fine} = 0.4V_{gap}, V_{fine} = 0.5V_{gap}, and so on, until the gaps are fully filled.
4. Gradually reduce the sand content in the mixed soil by controlling the quality of sand particles (M_{sand} = 0.9M_{0sand}, M_{sand} = 0.8M_{0sand}, M_{sand} = 0.7M_{0sand}, and so on), while the remaining volume is filled with fines.

The sample preparation plan for mixed soil with varying particle sizes and fine content is detailed in Table 2. This article focuses on the contact interface between particles in mixed soil. Compared to the mass fraction, the volume fraction can better represent the number of contact surfaces between sand particles and fine particles. So, the fine particle content (FC) in this study is expressed as a volume ratio (V_{fine}/V).

Considering the inherent water content of soil in its natural state, and the characteristics of the particle surface of bentonite are gradually displayed after absorbing water, so the fine particles in this article are bentonite with a certain water content. The research focus of this article is on the effects of content, particle size, and mineral composition on the contact interface between particles. Therefore, there is not much discussion on the water content of fine particles. However, considering the feasibility of sample preparation and the role of fine particle surface, this experiment chooses a water content of 50% for fine particles. Bentonite is prone to swelling and agglomeration after absorbing water, which can affect sample preparation. To eliminate these effects, this experiment adopts the unsaturated sample preparation method. Firstly, add 47% water to the dry bentonite and stir evenly. Then, seal and let the bentonite fully absorb water and expand. Then, use a 1–2 mm sieve to screen out small moist particles and test the water content. Based on the water content tested, spray a certain amount of water to reach 50% of the water content, and let it sit overnight.

Subsequently blending the prepared fines uniformly with sand according to predetermined proportions. Subsequently, the mixture is compacted within a ring knife using a consistent striking method, ensuring uniform energy application for each strike. An illustration of the prepared sample is presented in Figure 3A. Following the preparation of samples, they are carefully enclosed with plastic wrap alongside the ring knife. These wrapped samples are then placed within a controlled environment with constant temperature and humidity conditions, allowing them to stand undisturbed for a duration of 24 h. This resting period facilitates the establishment of a stable soil state within the samples.

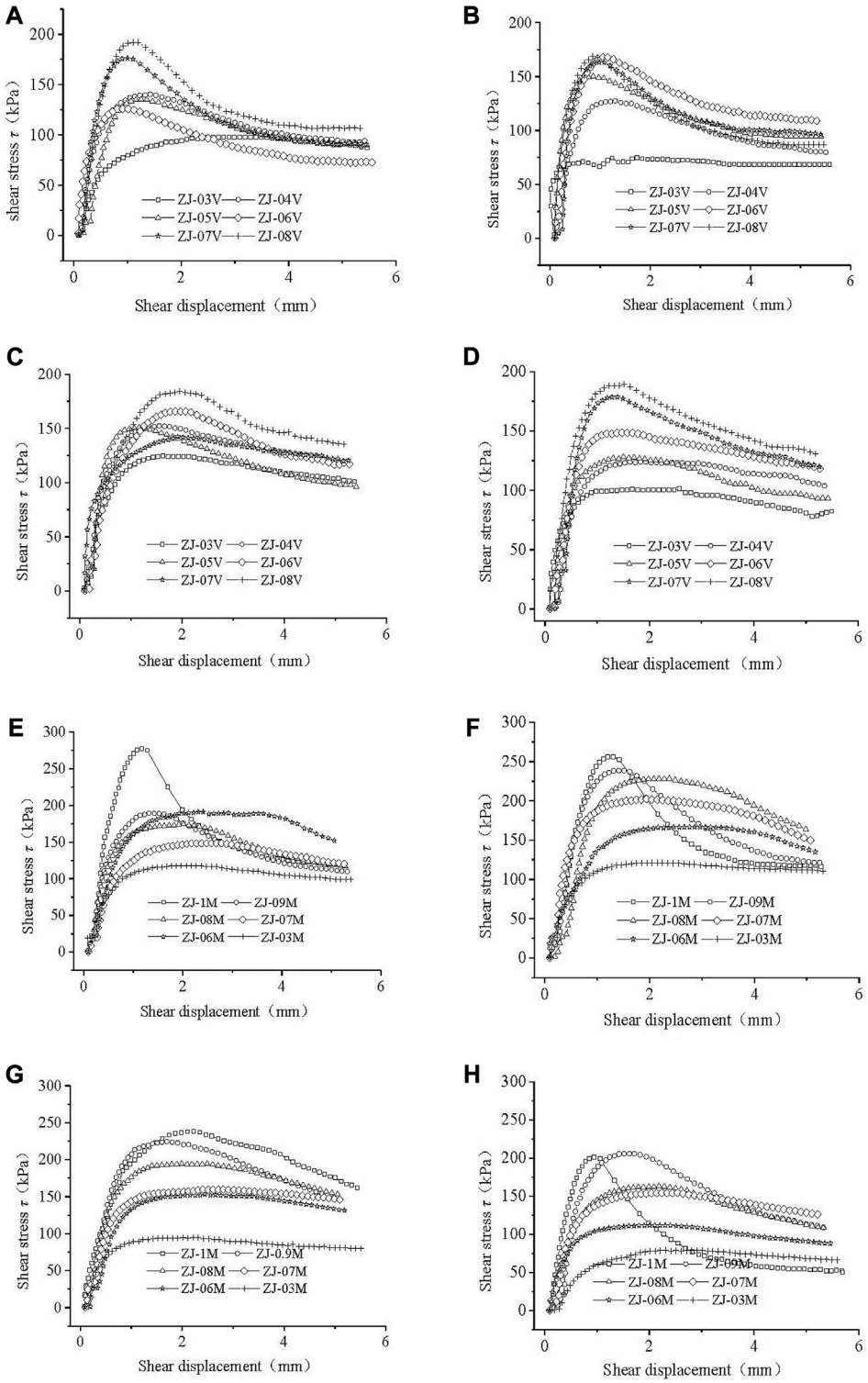

FIGURE 4
Relationships between shear stress and shear displacement of mixed soil samples (p = 150 kPa). **(A)** D_{sand} = 0.5 mm; **(B)** D_{sand} = 0.7 mm; **(C)** D_{sand} = 0.9 mm; **(D)** D_{sand} = 1.5 mm; **(E)** D_{sand} = 0.5 mm; **(F)** D_{sand} = 0.7 mm; **(G)** D_{sand} = 0.9 mm; **(H)** D_{sand} = 1.5 mm.

Subsequent to the resting period, the samples undergo direct shear testing in accordance with the specifications outlined in Table 2. The experimental apparatus employed for the direct shear tests is the strain-controlled direct shear instrument, as depicted in Figure 3B. Throughout the direct shear experiments, the vertical load is consistently controlled at values of p = 100kPa, p = 150kPa, p = 200kPa, and p = 250kPa, while the shear rate remains maintained at 0.8 mm/s. It is essential to highlight that both

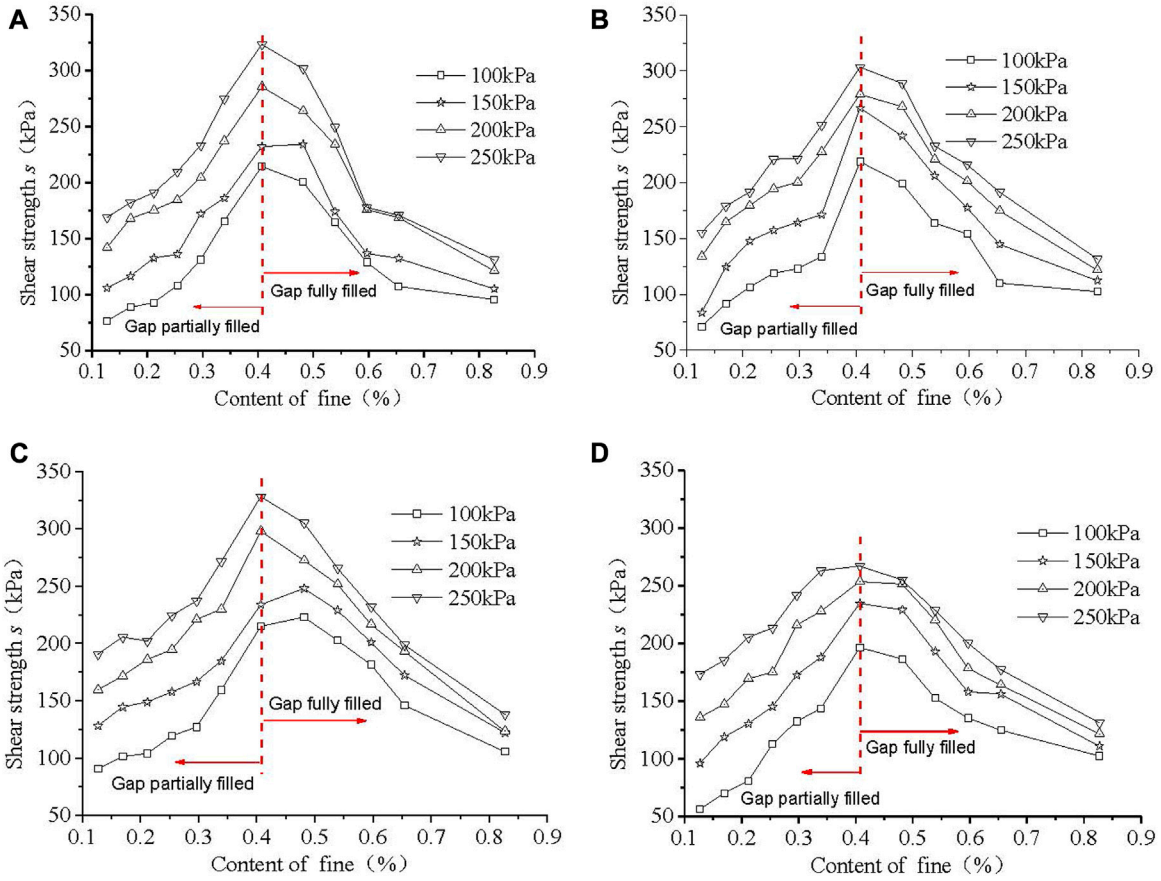

FIGURE 5
Shear strength of the sample with different FC. **(A)** D_{sand} = 0.5 mm; **(B)** D_{sand} = 0.7 mm; **(C)** D_{sand} = 0.9 mm; **(D)** D_{sand} = 1.5 mm.

the sample preparation and the execution of the direct shear tests are carried out meticulously in adherence to relevant standards (ASTM: D420 – D5876/D5876m), ensuring the accuracy and reliability of the results obtained.

2.2 Test results

(1) Relationship between shear stress and shear displacement

The interplay between shear stress and shear displacement provides insights into various soil properties during the shearing process. Due to the extensive range of experimental groups, only samples subjected to a vertical pressure of p = 150 kPa are illustrated in Figure 4. From Figure 4, it can be seen that most specimens exhibit strain softening phenomenon during the shear process. The shear stress-shear displacement curves for these samples highlight a general trend of initial increase followed by decrease, with the rate of decrease gradually diminishing until the curve levels off.

Shear strength, a vital parameter, is characterized by peak shear stress as well as strength indices such as cohesive force (c) and friction angle (φ). Figure 5 presents the peak shear strength of samples with varying sand particle sizes and FC, obtained from the experiment.

Additionally, the shear strength indices, including cohesive force and friction angle, are depicted in Figure 6.

Figure 5 reveals a distinct pattern in the shear strength of soil mixtures concerning FC. An increase and subsequent decrease in shear strength is observed with varying FC values. Specifically, when the gaps between sand grains are partially filled, shear strength increases progressively with rising FC. However, after complete filling of these gaps, shear strength decreases as FC continues to increase. Furthermore, it is notable that under identical conditions, greater vertical pressures correspond to higher shear strengths in the soil.

2.3 Result analysis

The mechanical behavior of soil is intricately tied to the fundamental properties of particles and the resultant soil structure. For instance, the honeycomb structure formed by clay particles translates to elevated porosity and reduced engineering bearing capacity, while the densely packed arrangement of gravel and fine clay particles offers greater bearing capacity. In the context of mixed soil, the interplay between fine and coarse particles adheres to specific rules, yielding a diversity of structural configurations. The transmission of forces and coordination of deformations among soil

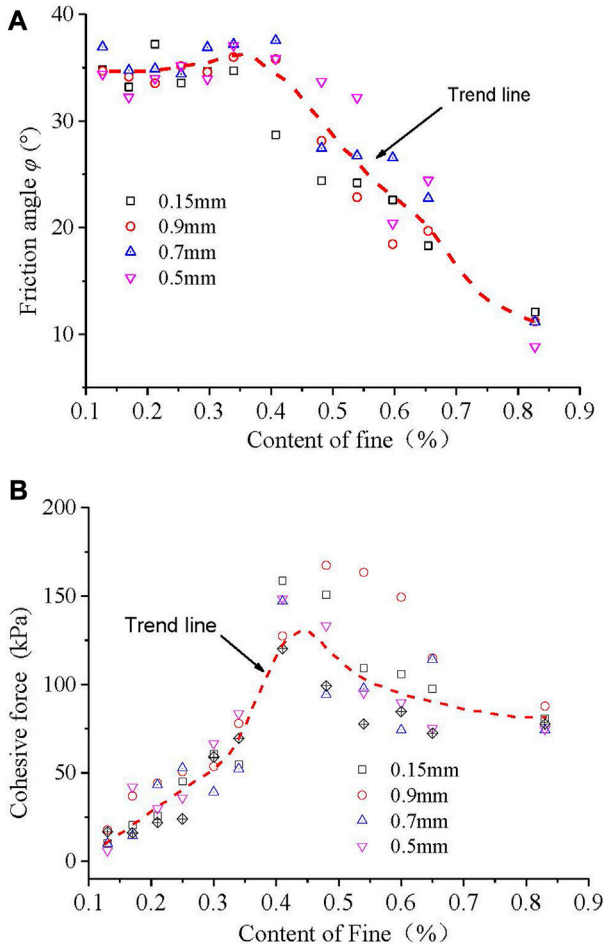

FIGURE 6
The cohesive force and friction angle of the sample with different sand diameters and FC. **(A)** Variation of friction angle of mixed soil; **(B)** Variation of the cohesive force of mixed soil.

particles occur via contact interfaces. Concurrently, particle surface properties significantly influence soil structure formation. For instance, fine clay particles exhibit relatively thick water absorption films on their surfaces, facilitating the development of a honeycomb structure. In contrast, the electric double layer on sand and gravel particles' surfaces is notably thin, promoting denser structures.

Consequently, the outcomes of our conducted tests can be elucidated through the lens of particle contact interfaces within the microstructure of mixed soil. In the case of pure sand, the particle contact involves rigid interactions, leading to pronounced friction effects when particles undergo relative movement, as illustrated in Figure 7A. Conversely, pure clay particles possess thicker adsorbed water films on their surfaces, primarily resulting in soft particle contacts and generating cohesion effects during relative particle movement.

Mixed soil, comprised of larger sand particles and smaller clay particles, engenders intricate contact scenarios. Here, particle contacts are diverse, encompassing hard contacts between sand particles, soft contacts among fine particles, and hybrid contacts between sand and fine particles, as depicted in Figure 7B. This complex interplay contributes to the mixed soil's mechanical behavior.

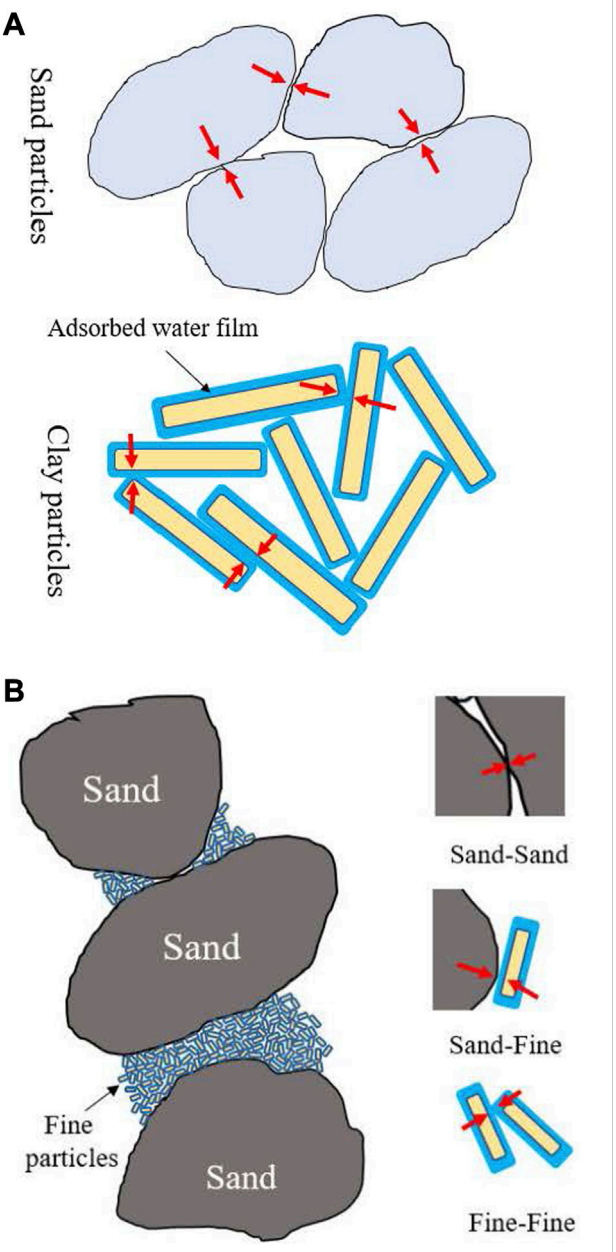

FIGURE 7
Contact interface of particles in mixed soil. **(A)** Surface and contact surface of different particles; **(B)** Mixed soil of clay fines with sands.

In conclusion, the diverse mechanical behavior exhibited by mixed soil samples in our study is inherently tied to the intricate contact interfaces formed between particles within the microstructure. The interplay between hard, soft, and mixed contacts contributes to the complex behavior observed during shear testing.

(1) Shear Stress-Shear Displacement Relationship

In our experiment, the particles established a relatively stable structure due to the 24-h resting period post-compaction. During the initial stages of shear, when the displacement is minimal, particle

contacts undergo elastic deformation. Consequently, resistance between particles gradually escalates within the elastic range. With continued shear displacement, select sand contact points and fine particle surfaces begin exhibiting plastic deformation while preserving the initial contact structure. This phase is marked by increasing bearing capacity of contact surfaces.

As shear displacement further increases, the stable particle structure collapses, leading to disruption of force transfer platforms and heightened motion freedom for sand particles. This instability markedly reduces the bearing capacity. Consequently, the shear stress-shear displacement curve transitions from an increasing phase to a decreasing one. Subsequent to extensive particle displacement, the reduced motion space culminates in the formation of a new contact structure among particles. This fragile contact arrangement provides limited bearing capacity, leading to the plateau observed in the curve.

Furthermore, vertical pressure influences the contact structure within the mixed soil during shear. Greater vertical loads enhance soil compaction, thereby amplifying the contact area and strength between particles. This effect is evidenced by the overall increase in shear strength with heightened vertical pressure.

(2) Influence of Mineral Composition

The shearing process highlights distinct stress and deformation behaviors between sand and fine clay particles. Fine clay particles, possessing an extensive specific surface area and considerable negative surface charges, tend to develop thicker adsorbed water films. Consequently, contact between clay fines predominantly involves interactions between these water films, showcasing a pronounced cohesive effect. On the other hand, sand particles exhibit a smaller specific surface area, lower surface charge density, and minimal impact of adsorbed water films relative to their volume. Consequently, particle contacts within sand primarily entail direct interactions between quartz crystals, leading to pronounced frictional effects.

Throughout shear, relative displacement between fine clay particles results in cohesive force at contact surfaces. Meanwhile, rotational or translational displacement of sand particles triggers friction force among sand particles and cohesion force at the fine-sand interface. This combination of cohesive and frictional forces at contact interfaces contributes to the macroscopic cohesive and frictional bearing capacities of mixed soil. Notably, the cohesive bearing capacity increases with rising FC (Figure 6).

(3) Influence of Content

Content, whether fines or sands, significantly influences mixed soil shear strength. When gaps between sand particles are partially filled, contacts primarily involve hard interactions, leading to larger friction angles (Figure 6A). Gradual increments in fines content introduce new contacts between fine-fine and fine-sand particles, contributing to increased cohesive force. Consequently, shear strength experiences a gradual rise within a FC range of 0.13–0.41 (Figure 5).

Upon complete gap filling, contact between sand particles diminishes with decreasing sand content and increasing FC. This leads to decreasing friction angles. Surprisingly, cohesion force does not continue increasing with higher fines content; instead, it decreases. High sand content and saturated fines reduce sand movement freedom, invoking internal crystal cohesion. Subsequently, cohesion within mixed soil relies on fines-fines, fine-sand, and internal crystal cohesion of sand, resulting in high cohesion. As fines content rises, cohesion diminishes due to reduced fine-sand cohesion and internal crystal cohesion. Hence, shear strength decreases as FC increases (Figure 5).

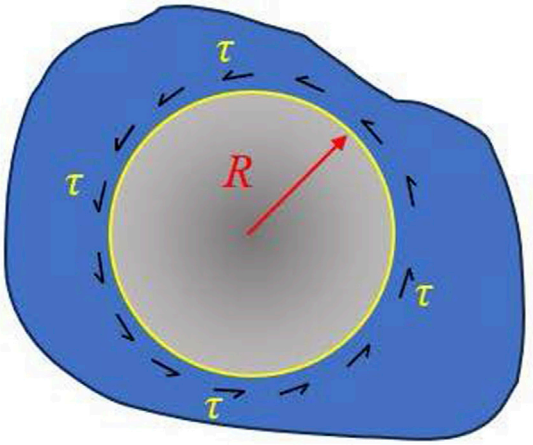

FIGURE 8
Schematic diagram of the rotational moment resistance of sand particles.

(4) Influence of Sand Particle Size

The experiment underscores the pivotal role of sand particle size. Sand particles mainly undergo rotational displacement during shear. Cohesive force exerted by fines generates shear stress on contact surfaces between sand and fines, restraining sand rotation and contributing to shear load capacity (Figure 8).

Assuming spherical particles with their centers as rotation centers, the anti-rotation moment exerted by fines on a single sand particle can be expressed as:

$$M = R \cdot S \cdot \tau \tag{1}$$

Where, R represents the particle radius, and S is the particle's surface area. For all particles, the collective anti-rotation moment of the particles becomes:

$$\sum M = \sum R \cdot S \cdot \tau = n \cdot \bar{R} \cdot S \cdot \tau \tag{2}$$

In the latter formula, $\bar{R}$ represents the average particle radius, n is the particle count which can be deduced from the total sand mass and the individual sand mass. This allows us to rewrite the formula as:

$$\sum M = \sum R \cdot S \cdot \tau = n \cdot \bar{R} \cdot S \cdot \tau = \frac{m}{\frac{4}{3}\pi \bar{R}^3 \rho} \cdot \bar{R} \cdot 4\pi \bar{R}^2 \cdot \tau = \frac{m\tau}{3\rho} \tag{3}$$

Within formula (3), m denotes the sand mass, and ρ signifies the sand density. The derivation of this equation underscores that, as

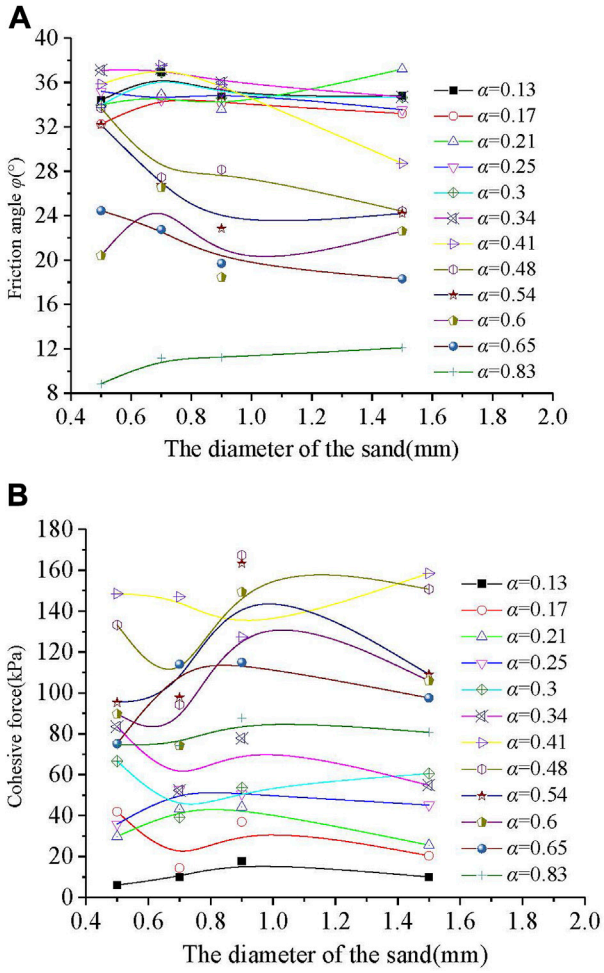

FIGURE 9
Influence of sand particle size on friction angle and cohesive force of mixed soil. **(A)** Particle size-friction angle; **(B)** Particle size-cohesive force.

long as the total sand mass in the mixed soil remains constant, sand particle size does not influence the mixed soil's shear strength.

In our experiment, Figure 9 illustrates the relationship between the shear strength indices of samples and the diameters of sand particles. The graph showcases varied trends, including decreasing strength indices with larger particle sizes, increasing indices, and inconsistent trends. Eq. 5 would suggest a linear relationship, but several factors could contribute to the observed deviation. Since the calculation formula simplifies particle shapes to standard spheres, real-world particle encapsulation by fines might not be guaranteed. This could potentially explain the lack of a consistent pattern in the curves within Figure 9.

3 Discussion on mechanism of mixed soil mechanics using multi-scale method

The previous analysis has demonstrated that factors such as particle composition, particle content, and other variables influence the mechanical properties of mixed soil through the contact interfaces between particles. However, a more detailed mechanism requires further exploration. In the realm of metals and nanomaterials, changes in particle size can alter surface properties, subsequently impacting the state of particle contact interfaces. The particles in mixed soil encompass a range of sizes, spanning multiple scales. As particle size diminishes, specific surface area and the ratio of fractured crystal bonds increase. Consequently, surface charges and adsorption energy on particle surfaces rise, resulting in more pronounced adsorbed water films. This phenomenon, in turn, affects the contact surfaces between particles. Simultaneously, the diverse mineral composition of particles in mixed soil contributes to distinct characteristics. Under the same particle size, clay particles exhibit considerably higher surface charge than non-clay particles, and the relative thickness of adsorbed water on clay particle surfaces exceeds that of non-clay particles. Consequently, contact interfaces between clay particles largely involve water film interactions, while contact interfaces between sand particles primarily constitute mineral crystal interactions. Evidently, the properties of particle surfaces and interfaces within mixed soil correlate with the relative thickness of adsorbed water films on particle surfaces. Moreover, this thickness is directly associated with the particle surface's adsorption capacity.

Chen and Tong, (2023) explored how clay particles possess heightened electric field forces, whereas sand particles exhibit stronger van der Waals forces. Leveraging these insights within an energy multi-scale framework (Chen and Tong, 2023), the current study adopts van der Waals and electric field forces to represent particle friction and adsorption energies, respectively. This is encapsulated in the following equations:

$$F = \alpha(F_e + F_w)_B + \beta(F_e + F_w)_S \tag{4}$$

Here, F denotes particle microforces, Fe signifies Coulomb force, Fw represents van der Waals force, B designates bentonite (fines), and S stands for sand. Concretely:

$$F_e = \frac{1}{4\pi\varepsilon_0}\frac{q_1 q_2}{r^2}; G = \rho g V = \rho g \pi d^3/6; F_w = \frac{Ad}{24H^2} \tag{5}$$

Within the above equation, represents vacuum permittivity, q1 and q2 denote particle charge, r signifies particle center distance, ρ indicates particle density, d represents particle diameter, A corresponds to the Hamaker constant, and H stands for particle net distance. Specific parameter values can be extracted from pertinent literature (Chen and Tong, 2023), with microforces calculated for all samples. The computed outcomes, alongside shear strength derived from testing, are visually depicted in Figure 10.

Figure 10 unmistakably illustrates the consistent relationship between particle force F and fines content, mirroring the effect of fines content on mixed soil shear strength. This congruence substantiates the employment of particle microforces as a plausible explanation for the mechanical behavior of mixed soils.

4 Conclusion

In this paper, the analysis of the mechanical behavior of mixed soil is conducted through direct shear experiments. The initial explanation of the mixed soil's mechanical behavior is provided

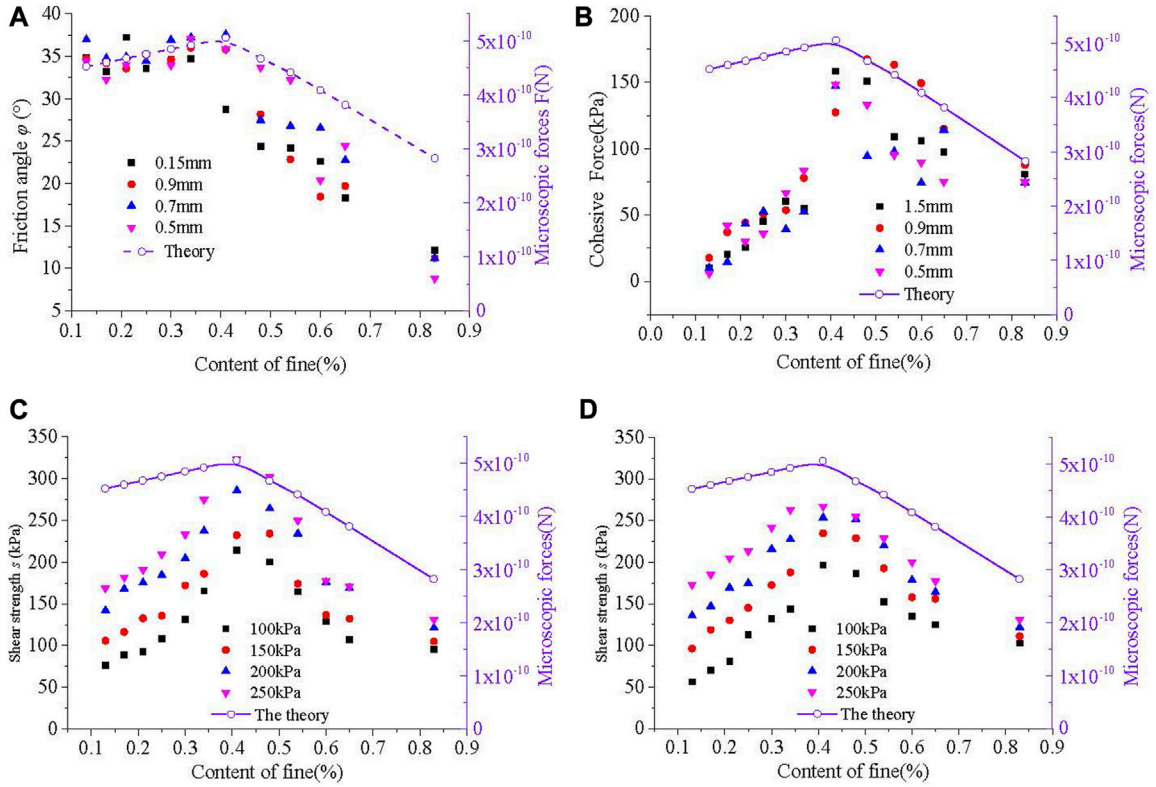

FIGURE 10
Variation of microscopic forces and shear strength with fines content. **(A)** The microscopic forces *F*-friction angle φ; **(B)** The microscopic forces *F*-cohesive force *c*; **(C)** The microscopic forces *F* -shear strength *s* (*d* = 0.5 mm); **(D)** The microscopic forces *F* -shear strength *s* (*d* = 1.5 mm).

by considering the contact surfaces between particles. Subsequently, the discussion delves into the mechanics through the lens of microscopic adsorption energy of particles. This comprehensive research leads to the formulation of four primary conclusions:

(1) Effect of Fine Particle Content: The strength of mixed soil is influenced differently by the content of fine particles under various filling states. When the gap between particles is partially filled, increasing the fine particle content enhances the strength of the mixed soil. However, when the gap is completely filled by fines, an increase in fine particle content leads to a gradual decrease in the strength of the mixed soil.

(2) Role of Particle Composition: Different types of particles contribute distinctively to the strength of the mixed soil. Larger sand particles predominantly contribute to frictional effects, where the friction angle gradually diminishes as sand content decreases. Clay fines primarily contribute to cohesive effects, while also restraining sand displacement, thereby enhancing the friction angle and cohesive force of the mixed soil.

(3) Impact of Particle Size: Particle size of sand particles, when holding mass constant, does not directly impact the strength of mixed soil. The anti-rotation moment of sand particles under shear load is influenced by factors such as particle surface area, size, cohesive contribution from fines, and particle count. This combined influence indicates that the shear strength of mixed soil does not exhibit a direct correlation with particle size.

(4) Microscopic Analysis: Microscopic considerations, specifically surface energy and interface contact of particles, effectively elucidate the mechanism behind the mechanical behavior of mixed soil. When the gap is partially filled, the cumulative microscopic force of particles increases with higher fine particle content. Conversely, under fully filled conditions, the cumulative microscopic force decreases with elevated fine particle content. This trend in the cumulative microscopic force curve of mixed soils aptly describes and predicts the relationships between shear strength and fine content, internal friction angle and fine content, and cohesion and fine content.

In essence, this study provides a nuanced understanding of how different factors at various scales contribute to the complex mechanical behavior of mixed soil. The combination of experimental investigation, theoretical analysis, and microscopic insights contributes to a comprehensive explanation of the observed behaviors.

Data availability statement

The original contributions presented in the study are included in the article/Supplementary Material, further inquiries can be directed to the corresponding author.

Author contributions

JC: Funding acquisition, Writing–original draft, Writing–review and editing, Methodology. JY: Data curation, Funding acquisition, Writing–review and editing. HT: Methodology, Supervision, Writing–review and editing. YF: Methodology, Supervision, Writing–review and editing. RG: Formal Analysis, Resources, Writing–review and editing.

Funding

The authors declare financial support was received for the research, authorship, and/or publication of this article. This research is supported by the Guangdong Basic and Applied Basic Research Foundation (Nos. 2022A1515110793 and 2023A1515030051).

Conflict of interest

The authors declare that the research was conducted in the absence of any commercial or financial relationships that could be construed as a potential conflict of interest.

Publisher's note

References

Allahyari, N., and Maleki, M. (2022). Investigation into small-strain shear modulus of sand-gravel mixtures in different moisture conditions and its correlation with static stiffness modulus. *Int. J. geotechnical Eng.* 16 (8), 962–973. doi:10.1080/19386362.2022.2033482

Amini, F., and Qi, G. Z. (2000). Liquefaction testing of stratified silty sands. *J. Geotechnical Geoenvironmental Eng.* 126 (3), 208–217. doi:10.1061/(asce)1090-0241(2000)126:3(208)

Bahadori, H., Ghalandarzadeh, A., and Towhata, I. (2008). Effect of non plastic silt on the anisotropic behavior of sand. *Soil Found.* 48 (4), 531–545. doi:10.3208/sandf.48.531

Bai, Bing, Zhou, Rui, Cai, Guoqing, Hu, Wei, and Yang, Guangchang (2021). Coupled thermo-hydro-mechanical mechanism in view of the soil particle rearrangement of granular thermodynamics. *Comput. Geotechnics* 137 (8), 104272. doi:10.1016/j.compgeo.2021.104272

Bobei, D. C., Lo, S. R., Wanatowski, D., Gnanendran, C. T., and Rahman, M. M. (2009). Modified state parameter for characterizing static liquefaction of sand with fines. *Can. Geotechnical J.* 46 (3), 281–295. doi:10.1139/t08-122

Carraro, J., Prezzi, M., and Salgado, R. (2009). Shear strength and stiffness of sands containing plastic or nonplastic fines. *J. Geotechnical Geoenvironmental Eng.* 135 (9), 1167–1178. doi:10.1061/(asce)1090-0241(2009)135:9(1167)

Chang, C. S., Yin, Z. Y., and Hicher, P. Y. (2010). Micromechanical analysis for interparticle and assembly instability of sand. *J. Eng. Mech.* 137 (3), 155–168. doi:10.1061/(asce)em.1943-7889.0000204

Chen, J., Tong, H., Yuan, J., Fang, Y., and Huang, X. (2023). Energy multi-scale method to analyze the scale effect of soil particles. *Front. Mater.* 10. doi:10.3389/fmats.2023.1137758

De Frias Lopez, R., Silfwerbrand, J., Jelagin, D., and Birgisson, B. (2016). Force transmission and soil fabric of binary granular mixtures. *Géotechnique* 66 (7), 578–583. doi:10.1680/jgeot.14.p.199

Gao, Y., Wang, Y. H., and Su, J. C. (2015). Experimental characterization of the influence of fines on the stiffness of sand with inherent fabric anisotropy. *Soils Found.* 55 (5), 1148–1157. doi:10.1016/j.sandf.2015.09.015

Gong, J., Nie, Z., Zhu, Y., Liang, Z., and Wang, X. (2019). Exploring the effects of particle shape and content of fines on the shear behavior of sand-fines mixtures via the DEM. *Comput. Geotechnics* 106, 161–176. doi:10.1016/j.compgeo.2018.10.021

Karakan, E. (2023). Flow index-liquid limit relationship by fall-cone tests in clay-sand mixtures. *Eng. Sci. Technol. Int. J.* 41, 101405. doi:10.1016/j.jestch.2023.101405

Ke, X., Chen, J., and Shan, Y. (2019). A new failure criterion for determining the cyclic resistance of low-plasticity fine-grained tailings. *Eng. Geol.* 261, 105273. doi:10.1016/j.enggeo.2019.105273

Krim, A., Arab, A., Chemam, M., Brahim, A., Sadek, M., and Shahrour, I. (2017). Experimental study on the liquefaction resistance of sand–clay mixtures: effect of clay content and grading characteristics. *Mar. Georesources Geotechnol.* 37, 129–141. doi:10.1080/1064119x.2017.1407974

Lee, K. L., and Seed, H. B. (1967). Cyclic stress conditions causing liquefaction of sand. *ASCE Soil Mech. Found. Div. J.* 93 (1), 47–70. doi:10.1061/jsfeaq.0000945

Li, X., Liu, J., and Nan, J. (2022). Prediction of dynamic pore water pressure for calcareous sand mixed with fine-grained soil under cyclic loading. *Soil Dyn. Earthq. Eng.* 157, 107276. doi:10.1016/j.soildyn.2022.107276

Monkul, M. M., Etminan, E., and Şenol, A. (2017). Coupled influence of content, gradation and shape characteristics of silts on static liquefaction of loose silty sands. *Soil Dyn. Earthq. Eng.* 101, 12–26. doi:10.1016/j.soildyn.2017.06.023

Monkul, M. M., Kendir, S. B., and Tütüncü, Y. E. (2021). Combined effect of fines content and uniformity coefficient on cyclic liquefaction resistance of silty sands. *Soil Dyn. Earthq. Eng.* 151, 106999. doi:10.1016/j.soildyn.2021.106999

Monkul, M. M., and Ozden, G. (2007). Compressional behavior of clayey sand and transition fines content. *Eng. Geol.* 89 (3-4), 195–205. doi:10.1016/j.enggeo.2006.10.001

Monkul, M. M., and Yamamuro, J. A. (2011). Influence of silt size and content on liquefaction behavior of sands. *Can. Geotechnical J.* 48 (6), 931–942. doi:10.1139/t11-001

Park, S., and Kim, Y. (2013). Liquefaction resistance of sands containing plastic fines with different plasticity. *J. Geotechnical Geoenvironmental Eng.* 5 (139), 825–830. doi:10.1061/(asce)gt.1943-5606.0000806

Phan, Q. T., Bui, H. H., Nguyen, G. D., and Bouazza, A. (2021). Effect of particle rolling resistance on drained and undrained behaviour of silty sand. *Acta Geotech.* 16 (16), 2657–2682. doi:10.1007/s11440-020-01128-y

Polito, C. P., and Martin, J. R. (2001). Effects of nonplastic fines on the liquefaction resistance of sands. *J. Geotechnical Geoenvironmental Eng.* 5 (127), 408–415. doi:10.1061/(asce)1090-0241(2001)127:5(408)

Porcino, D. D., Diano, V., Triantafyllidis, T., and Wichtmann, T. (2020). Predicting undrained static response of sand with non-plastic fines in terms of equivalent granular state parameter. *Acta Geotech.* 2020 (15), 867–882. doi:10.1007/s11440-019-00770-5

Sabbar, A. S., Chegenizadeh, A., and Nikraz, H. (2017). Static liquefaction of very loose sand-slag-bentonite mixtures. *Soils Found. -Tokyo-* 57 (3), 341–356. doi:10.1016/j.sandf.2017.05.003

Shan, Y., and Ke, X. (2021). Reexamination of collapse failure of fine-grained soils and characteristics of related soil indexes. *Environ. Earth Sci.* 80 (11), 402. doi:10.1007/s12665-021-09678-4

Troncoso, J. H., and Verdugo, R. (1985). Silt content and dynamic behavior of tailing sands. *Proc. Icsmfe.*

Wei, X., and Yang, J. (2019). Characterizing the effects of fines on the liquefaction resistance of silty sands. *Soils Found. -Tokyo* 59 (6), 1800–1812. doi:10.1016/j.sandf.2019.08.010

Yamamuro, J. A., and Lade, P. V. (1998). Steady-state concepts and static liquefaction of silty sands. *J. Geotechnical Geoenvironmental Eng.* 124 (9), 868–877. doi:10.1061/(asce)1090-0241(1998)124:9(868)

Yao, Y., Li, J., Ni, J., Liang, C., and Zhang, A. (2022). Effects of gravel content and shape on shear behaviour of soil-rock mixture: experiment and DEM modelling. *Comput. Geotechnics* 141, 104476. doi:10.1016/j.compgeo.2021.104476

Yin, Z., Zhao, J., and Hicher, P. Y. (2014). A micromechanics-based model for sand-silt mixtures. *Int. J. Solids Struct.* 51, 1350–1363. doi:10.1016/j.ijsolstr.2013.12.027

Zhu, Z., Zhang, F., Dupla, J. C., Canou, J., and Foerster, E. (2020). Investigation on the undrained shear strength of loose sand with added materials at various mean diameter ratios. *Soil Dyn. Earthq. Eng.* 137, 106276. doi:10.1016/j.soildyn.2020.106276

Zuo, K., Gu, X., Hu, C., Hu, J., and Gao, G. (2023). Shear stiffness of sand-fines binary mixtures: effects of sand gradation and fines content. *Constr. Build. Mater.* 383, 131364. doi:10.1016/j.conbuildmat.2023.131364